

MODELLING THE ALTERATION HALO OF A DIORITE INTRUSION.

Stephen P. White¹ and Bruce W. Christenson²

¹Applied Mathematics, Industrial Research Limited, Lower Hutt, N.Z.

²Institute of Geological and Nuclear Wairakei Research Centre, Sciences, New Zealand

Key Words water-rock interaction, reactive transport, two-phase chemical modelling, diorite

ABSTRACT

A model is presented of a hydrothermal reservoir containing a reactive fluid dominated by CO_2 . We then consider the effect of a pulse of magmatic vapour into the base of this reservoir, and calculate the changed chemical and physical conditions as the reservoir is allowed to evolve for 15,000 years. The chemistry in the reservoir is described by eleven component species, H_2O , H^+ , Cl^- , $\text{SO}_4^{=}$, HCO_3^- , HS^- , SiO_2 , Al^{+++} , Ca^{++} , K^+ and Na^+ . Associated with these components are 32 secondary species, nine minerals and four gases.

1. INTRODUCTION

Magmatic intrusions are obvious heat sources for geothermal fields. Perhaps the most thoroughly studied intrusion is that at the Kakkonda reservoir in Japan (Sasada et al 1998). Although less well studied, a diorite intrusion was also intersected during the drilling of geothermal well NM4 in the Ngatamariki field, New Zealand. This is to date the only in situ plutonic rock encountered in the Taupo Volcanic Zone (TVZ). There is extensive hydrothermal alteration both within the intrusion and in a halo surrounding the intrusion which suggests it acted as a heat source for the convective hydrothermal system active at the time (Christenson et al 1997, 1998).

White and Christenson (1998) modelled the rock alteration about such an intrusion using the reactive transport simulator CHEM-TOUGH2 (White 1995). In the present study, we remove one of the major assumptions of our earlier work, that of a single phase reservoir. Here we include the effect of dissolved gases on saturation pressure and include the major gases (CO_2 , H_2S , HCl and SO_2) as components in the gas and liquid phases.

2. MODEL DESCRIPTION

Drilling at Natamariki intersected a 700 ka old diorite intrusion at about two kilometres below the surface (Fig. 1). We have adopted a similar shallow-intrusion scenario in our model, and consider the thermal and chemical effects on the hydrothermal system immediately after emplacement.

We have adopted a cylindrical symmetry for the model. The cylinder has a radius of two kilometres, and extends from the surface to two kilometres depth. At the surface we assume water containing no dissolved solids or gases, a pH of 7, a constant temperature of 20°C and a pressure of one bar. On the vertical boundary of the model we assume hydrostatic pressures and temperatures consistent with a temperature gradient of 40°C/km. Fluid on the boundaries is in equilibrium with the rocks which are assumed to make up the unaltered reservoir. No fluid or heat flow is possible across the base of the model except over a central circular region of radius 450 metres at the base where various chemical components enter the modelled region from the degassing intrusion.

The modelled region is divided into ten horizontal layers each with a thickness of 200 metres. Each layer is divided into 20 'ring' elements. These elements are smallest near the center of the model and larger towards the boundaries. The upper 200 metres of the reservoir forms a partial cap and has a permeability of 0.01 milli-Darcy. The rest of the reservoir has a permeability of 1.0 milli-Darcy and porosity throughout is 0.1.

Modelling the transport of reactive chemicals is a computer intensive activity, and requires that a balance be struck between chemical complexity and calculation time. For this model, we have adopted a simplified subset of reservoir component species, including H_2O , H^+ , Cl^- , $\text{SO}_4^{=}$, HCO_3^- , HS^- , SiO_2 , Al^{+++} , Ca^{++} , K^+ and Na^+ . These fluid components allow the modelling of reactions between the main magmatic volatiles (CO_2 , SO_2 , H_2S , HCl) and the most common rock-forming minerals (albite, anorthite, K-feldspar and quartz). Absent from this mineral assemblage are iron-bearing phases which, as discussed below, exert an additional redox control on the fluid composition.

Simplifying assumptions adopted in the treatment are:

- chemical equilibrium is maintained;
- reservoir permeability is isotropic (fracture flow is ignored).
- only 10% of the rock mass is allowed to react with fluids, thus simulating the effect of fracture flow.

Whereas we believe the assumption of chemical equilibrium to be justified in the hot area of the reservoir, this assumption is certainly invalid in the cool areas. For example, the pH in the cool surface waters is much higher than normally found, but is correct for the interaction between pure water and the assumed rock assemblage at 20°C. Fluid flow within a geothermal reservoir is predominantly in (micro)fractures and not all the rock volume will be available for reaction with the reservoir fluid, we have taken the somewhat arbitrary value of 10% of the rock mass being available for reaction. The rock constituents act as a pH buffer to the acidic fluid formed when magmatic gas dissolves in the groundwater. Changing the amount of rock available for reaction will change the timescale over which this buffering lasts. This, and the other simplifications herein, will be addressed in future refinements of the model.

3. MAGMATIC INTRUSION

The fluxes of magmatic inputs into the convecting reservoir overlying the intrusion have been normalised to an inter-eruptive SO_2 flux of 350 t/d from White Island, as given in Table 1 in the row labeled 'full model'. These gases, with an enthalpy of steam at 350°C, are injected into the model over the source area for a period of three years. After this the rate is dropped to 1% of the initial rate and the simulation run to a final time of 15,000 years.

4. CHEMICAL ENVIRONMENT

The hydrothermal environment within or immediately adjacent to shallow (< 4km) cooling diorite plutons is characterised by high temperatures (up to 1100°C), pressures ranging from

hydrostatic to lithostatic (ca. 200 – 1000 bar), and by the presence of highly reactive fluids. Here we consider only the interaction between the volatile species released from a cooling magma, and the overlying hydrothermal environments. This is in keeping with evidence from Ngatamariki suggesting that release of magmatic volatiles occurred periodically during the cooling history of the diorite intrusion found there.

Fluid-rock reaction pathways which are typical of these environments are summarised in **Fig 2**. Using the reaction path simulation program REACT (Bethke, 1992), we have numerically titrated 900g of our simplified mineral assemblage (**Table 2**, and including 0.2 mole FeO) into 1 kg of condensed fumarolic discharge from White Island (fumarole #3, Gigganbach and Sheppard, 1989).

The fluid becomes progressively acid-neutralised and reduced as a result of the ensuing hydrolysis reactions. Early-formed alteration minerals include cation-stripped silicates (pyrophyllite at $T >$ ca. 290 °C, kaolinite at $T <$ 290 °C), sulfate minerals and elemental S, an assemblage typically found in active volcanic-hydrothermal systems (eg. Christenson and Wood, 1993). Later-formed minerals include albite, illite (muscovite) and calcite which are typical of gas-rich geothermal systems in the TVZ (Browne, 1989). The declining $\text{SO}_2(\text{g})/\text{H}_2\text{S}(\text{g})$ ratio and increasing $f\text{H}_2(\text{g})$ shows the reducing effect which water-rock interaction has on the oxidation state of the fluid, although the coexistence of hematite and pyrite in the late alteration assemblage points to a still somewhat elevated oxidation state of the fluid relative to production discharges in the TVZ (Browne, 1998).

Extending this chemical approach to a reservoir-wide model, whilst maintaining a real sense of time and space (i.e. relevance to TVZ systems) required that the CHEM-TOUGH2 model be done in a series of steps. Firstly, the initial pressure and temperature state of the reservoir was calculated using only the TOUGH2 simulator (Pruess, 1987). Starting with a reservoir at 20°C and hydrostatic pressures the model was run with the source terms specified in **Table 1** for the scenario labeled 'initial' until a steady state was reached.

This calculation provided starting temperature and pressure conditions for the second calculation. The aim was to estimate chemical conditions and rock alteration products in a single-phase liquid reservoir containing CO_2 and the initial mineral assemblage (**Table 2**). The heat and mass flows into the reservoir during this run equate to a source fluid containing 3.6% CO_2 by weight (Table 1). This model was run to simulate the evolution of the reservoir for 100,000 years. The temperatures, pressures aqueous chemical components and mineral assemblage at the end of this simulation provided the initial state of the reservoir prior to intrusion of the diorite.

5. RESULTS

Results of the modelling are summarised in **Figs. 3-17**. Selected fluid parameters (i.e. pH, Cl^- and $\text{SO}_2/\text{H}_2\text{S}$, **Figs. 3-6**) depict the shape of the convective upwelling over the intrusion. As described above, hydrogen ions within the plume are consumed in hydrolysis reactions, and after 15,000 years, the distribution of Cl^- in the system shows that the cell has accomplished about one complete convective cycle. $\text{SO}_2/\text{H}_2\text{S}$ ratios show the fluids near the heat source to be most oxidising. Initial and final albite and anorthite (**Figs. 7-10**) show the extent of the hydrolysis reactions in the reservoir

after addition of the magmatic volatiles, as does the distribution of their reaction products kaolinite, pyrophyllite and muscovite (**Figs. 11-14**). Elemental S and alunite form in the low pH and oxidised environment close to the intrusion (**Figs. 15 and 16**). Similarly, Ca^{++} released from the increased dissolution of anorthite is taken up in anhydrite in the low pH zone close to the heat source, and calcite further away.

6. DISCUSSION and CONCLUSIONS

We have demonstrated that it is possible, with the assumptions given earlier, to model the chemical changes that take place in a geothermal reservoir in response to a large pulse of magmatic vapour. The chemical modelling includes sufficient detail to represent the processes associated with the neutralisation of the low pH fluids that result from the dissolution of magmatic vapour into reservoir fluid. The reactive transport approach described herein has implications for future geothermal exploration and development. Not only does it provide a predictive capability for "fitting" observed fluid chemistry and alteration products in shallow reservoir environments to unexplored heat source environments at depth, but also ultimately it will allow for testing production scenarios in near heat-source environments.

7. ACKNOWLEDGEMENTS

This paper was prepared using financial support from New Zealand Foundation for Research Science and Technology. We thank Warwick Kissling for his critical reading of the manuscript and useful comments.

8. REFERENCES

Bethke, C., (1992): The Geochemists Workbench; A user's guide to Rxn, Act2, Tact, React and Gtplot. Univ. Illinois, 213 p.

Browne PRL, (1998): Hydrothermal alteration in New Zealand geothermal systems. *Proc. 9th Int. Sym. On Water-Rock Interaction*. (Arehart and Hulston (eds) Balkema (Pub.), p 11-18.

Christenson, B.W., Wood, C.P., Arehart, G.B. (1998): Shallow magmatic degassing: Processes and PTX constraints for paleo-fluids associated with the Ngatamariki diorite intrusion, New Zealand. *Proc. 9th Int. Sym. On Water-Rock Interaction*. (Arehart and Hulston (eds) Balkema (Pub.) 1998.

Christenson BW, Mroczek EK, Wood CP, and Arehart GB (1997): Magma-ambient production environments: PTX constraints for paleo-fluids associated with the Ngatamariki diorite intrusion. In *Proc. 19th Geoth. Workshop*, p87-92 1997.

Gigganbach WF, Sheppard, DS (1989): Variations in temperature and chemistry of White Island fumarole discharges 1972-85. *NZ Geol Surv Bull* 103: 119-126 1998

Headenquist, J.W., Lowenstern, J.B. (1994): The role of magmas in the formation of hydrothermal ore deposits. *Nature* 370 August 1994

Pruess, K. (1987): TOUGH User's guide , Lawrence Berkeley Laboratory report LBL-20700 1987.

Sasada, M., Doi, N., Muffler, L.J.P., Hedenquist, J.W.(eds) (1998): Deep Geothermal Systems Japanese National project at Kakkonda. *Geothermics* 27 5/6 1998

White, S. P., (1995): Multiphase non-isothermal transport of systems of reacting chemicals, *Water Resour. Res.*, 31, 1761-1772, 1995.

White, S.P. and Christenson B.W. (1998): Modelling the alteration halo of a diorite. *Proc 20th Geoth. Workshop* p 127-132 1998

Table 1: Heat and mass flows for the three modelled scenario

Scenario	Heat Flow above intrusion (W/m ²)	H ₂ O (kg/sec)	H ⁺ (kg/sec)	HCO ₃ ⁻ (kg/sec)	HS ⁻ (kg/sec)	SO ₄ ⁼ (kg/sec)	Cl ⁻ (kg/sec)
Initial	2.0	0.54	0.0	0.0	0.0	0.0	0.0
CO ₂ only	2.0	0.54	3.17e-4	1.94e-2	0.0	0.0	0.0
Full model	2.0	152.5	1.33	59.79	2.77	12.87	2.47

Table 2: Initial rock composition

Name	Composition	Weight %
Albite	NaAlSi ₃ O ₈	40
Anorthite	CaAl ₂ Si ₂ O ₈	40
K-Feldspar	KAlSi ₆ O ₈	6
Quartz	SiO ₂	14

Table 3: Rock alteration products included in the calculations

Name	Composition
Alunite	K Al ₃ S ₂ O ₁₄
Anhydrite	CaSO ₄
Calcite	CaCO ₃
Kaolinite	Al ₂ Si ₂ O ₅ (OH) ₄
Muscovite	KAl ₂ (AlSi ₃ O ₁₀)(OH) ₂
Pyrophyllite	Al ₂ Si ₄ O ₁₀ (OH) ₂
Sulfur	S

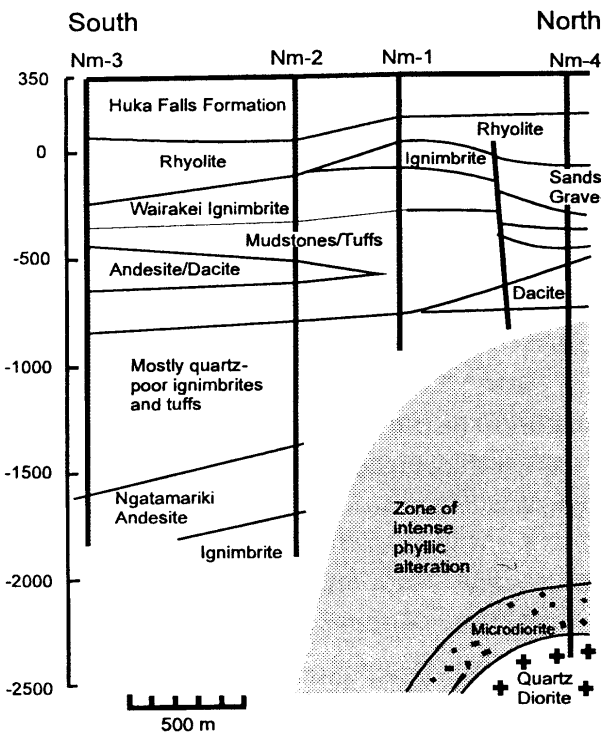


Figure 1: Geologic cross-section through four exploration wells at Natamariki (from Christenson *et al.*, 1998)

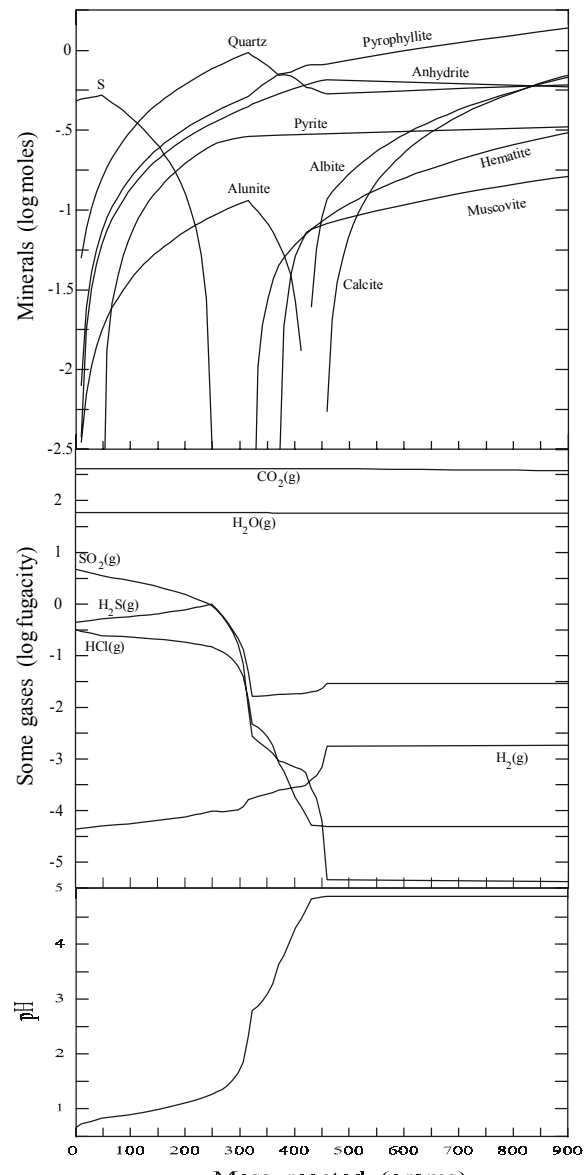


Figure 2: Reaction pathway resulting from titration of 900 g of the simplified mineral assemblage (including FeO) into 1 kg of White Island fumarolic condensate. Calculated at 300 °C.

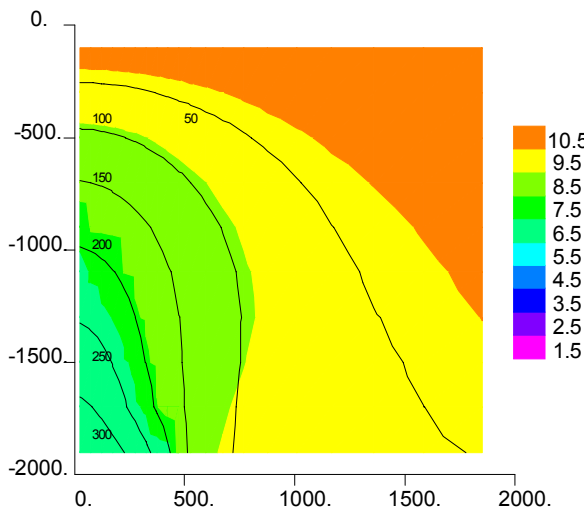


Figure 3: Initial pH, temperature (°C) is shown by labeled contours

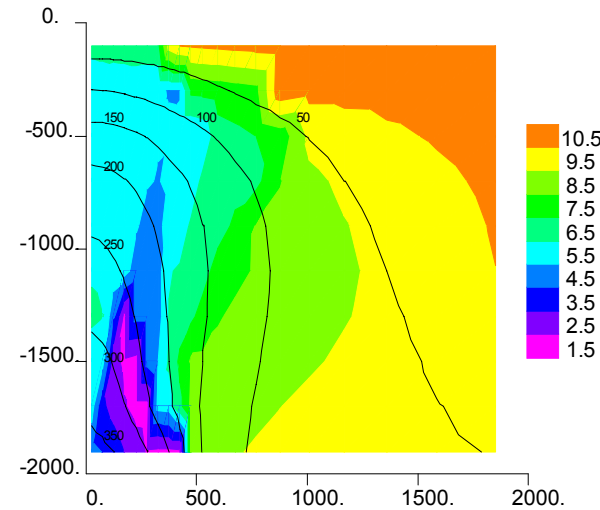


Figure 4: pH at 15,000 years, temperature (°C) is shown by labeled contours

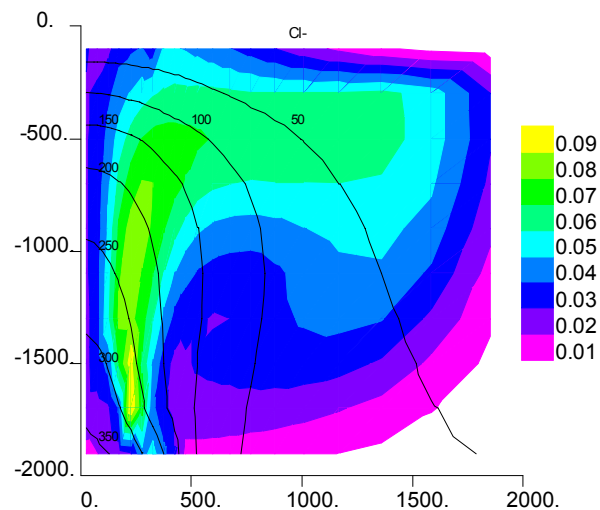


Figure 5: Cl^- concentration (M) at 15,000 years, temperature (°C) is shown by labeled contours.

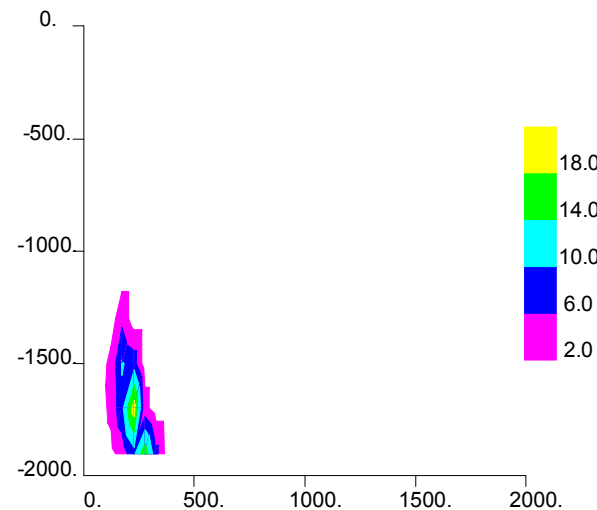


Figure 6: Ratio of partial pressures of SO_2 and H_2S ($\text{SO}_2/\text{H}_2\text{S}$) at 15,000 years

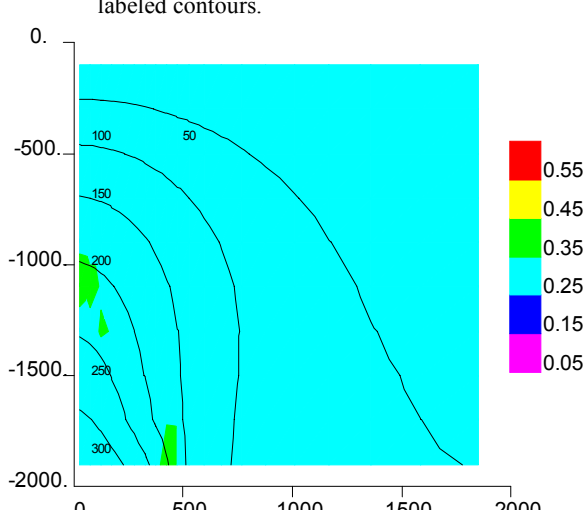


Figure 7: Initial albite distribution, temperature (°C) is shown by labeled contours. Units are moles/dm³ of fluid

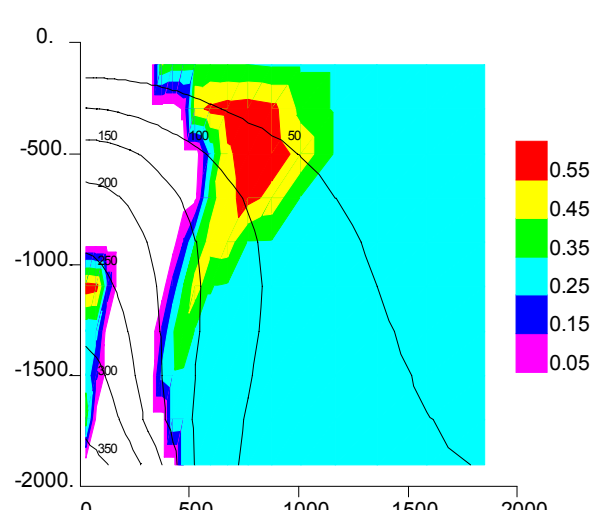


Figure 8: Distribution of albite at 15,000 years, temperature (°C) is shown by labeled contours. Units are moles/dm³ of fluid

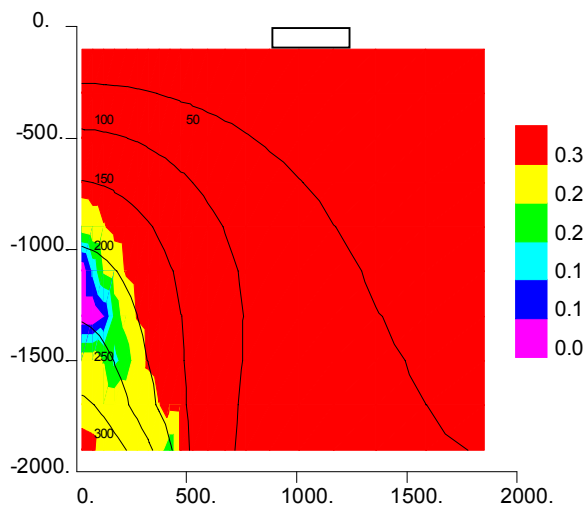


Figure 9: Initial anorthite distribution, temperature ($^{\circ}\text{C}$) is shown by labeled contours. Units are moles/dm 3 of fluid

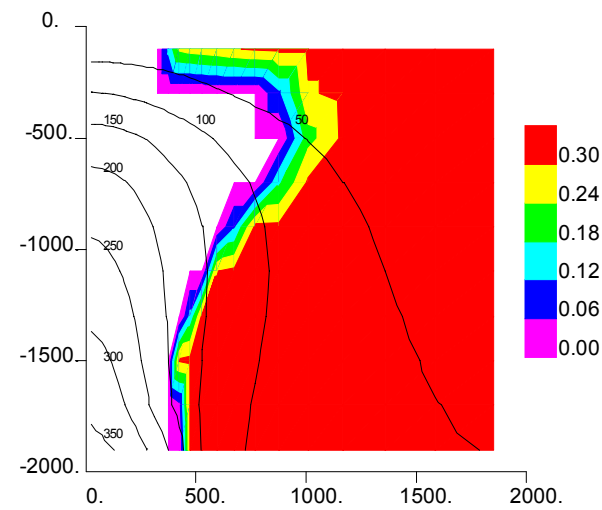


Figure 10: Anorthite distribution at 15,000 years, temperature ($^{\circ}\text{C}$) is shown by labeled contours. Units are moles/dm 3 of fluid

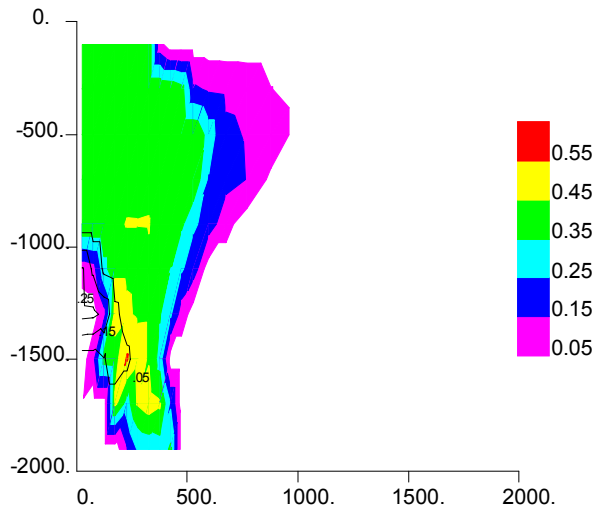


Figure 11: Kaolinite distribution at 15,000 years with initial values shown by labeled contours. Units are moles/dm 3 of fluid

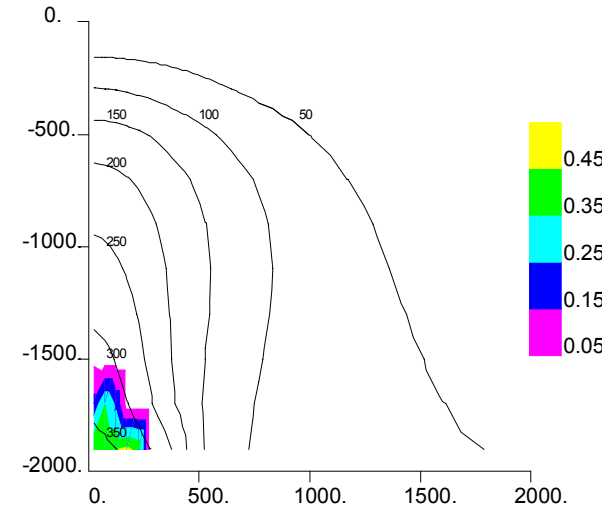


Figure 12: Pyrophyllite distribution at 15,000 years, with temperature values shown by labeled contours. Units are moles/dm 3 of fluid

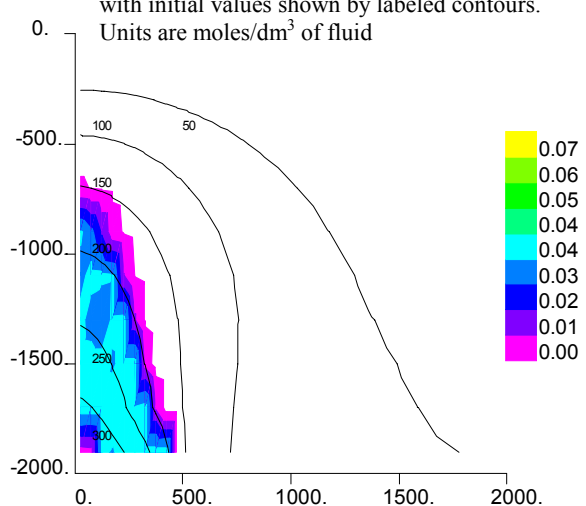


Figure 12: Initial muscovite distribution with temperature values ($^{\circ}\text{C}$) shown by labeled contours. Units are moles/dm 3 of fluid

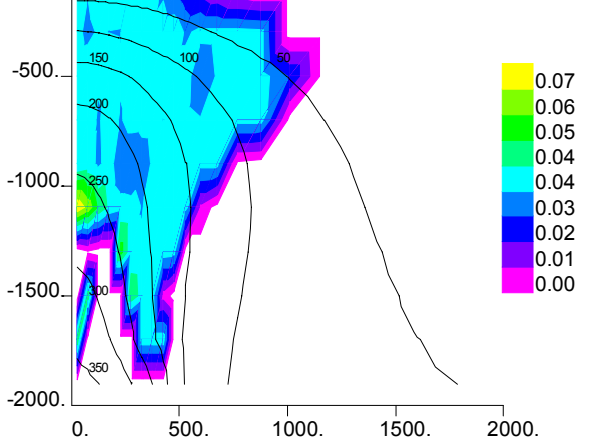


Figure 13: Muscovite distribution at 15,000 years with temperature values ($^{\circ}\text{C}$) shown by labeled contours. Units are moles/dm 3 of fluid

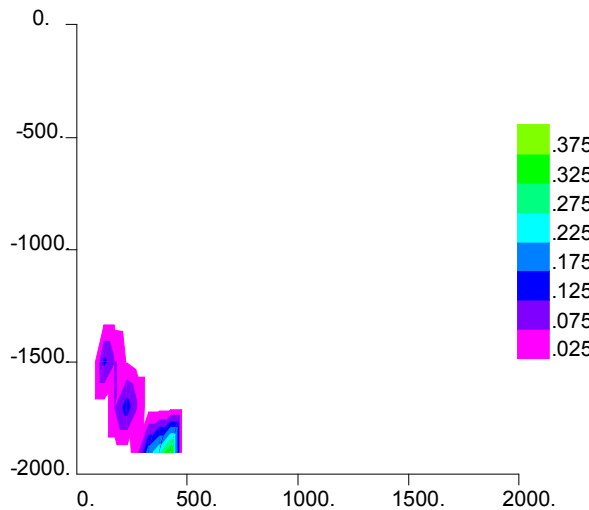


Figure 14: Native Sulfur distribution at 15,000 years
Units are moles/dm³ of fluid

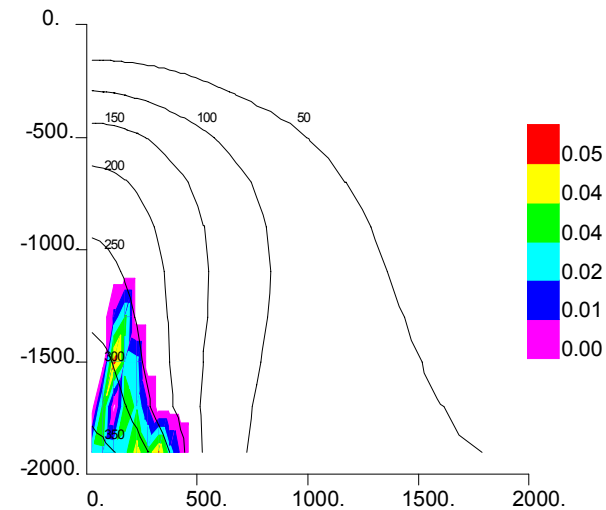


Figure 15: Alunite distribution at 15,000 years,
with temperature values (°C) shown by labeled
contours. Units are moles/dm³ of fluid

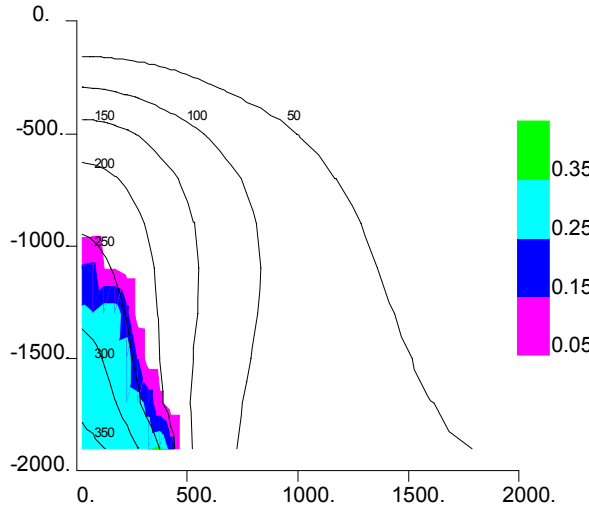


Figure 16: Anhydrite distribution at 15,000 years,
with temperature values (°C) shown by labeled
contours. Units are moles/dm³ of fluid.

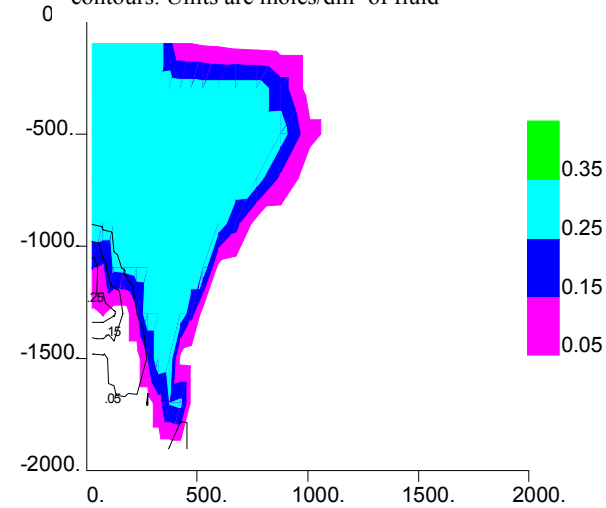


Figure 17: Calcite distribution with initial
distribution shown by labeled contours. Units are
moles/dm³ of fluid